



**Pacific Northwest**  
NATIONAL LABORATORY

*Proudly Operated by **Battelle** Since 1965*

# Effect of Silicon in U-10Mo Alloy

**August 2017**

EJ Kautz  
A Devaraj  
L Kovarik  
CA Lavender  
VV Joshi

## DISCLAIMER

This report was prepared as an account of work sponsored by an agency of the United States Government. Neither the United States Government nor any agency thereof, nor Battelle Memorial Institute, nor any of their employees, makes **any warranty, express or implied, or assumes any legal liability or responsibility for the accuracy, completeness, or usefulness of any information, apparatus, product, or process disclosed, or represents that its use would not infringe privately owned rights.** Reference herein to any specific commercial product, process, or service by trade name, trademark, manufacturer, or otherwise does not necessarily constitute or imply its endorsement, recommendation, or favoring by the United States Government or any agency thereof, or Battelle Memorial Institute. The views and opinions of authors expressed herein do not necessarily state or reflect those of the United States Government or any agency thereof.

PACIFIC NORTHWEST NATIONAL LABORATORY  
*operated by*  
BATTELLE  
*for the*  
UNITED STATES DEPARTMENT OF ENERGY  
*under Contract DE-AC05-76RL01830*

Printed in the United States of America

Available to DOE and DOE contractors from the  
Office of Scientific and Technical Information,  
P.O. Box 62, Oak Ridge, TN 37831-0062;  
ph: (865) 576-8401  
fax: (865) 576-5728  
email: [reports@adonis.osti.gov](mailto:reports@adonis.osti.gov)

Available to the public from the National Technical Information Service  
5301 Shawnee Rd., Alexandria, VA 22312  
ph: (800) 553-NTIS (6847)  
email: [orders@ntis.gov](mailto:orders@ntis.gov) <<http://www.ntis.gov/about/form.aspx>>  
Online ordering: <http://www.ntis.gov>



This document was printed on recycled paper.

(8/2010)

# **Effect of Silicon in U-10Mo Alloy**

EJ Kautz  
A Devaraj  
L Kovarik  
CA Lavender  
VV Joshi

August 2017

Prepared for  
the U.S. Department of Energy  
under Contract DE-AC05-76RL01830

Pacific Northwest National Laboratory  
Richland, Washington 99352



## Purpose and Scope

The purpose of this document is to provide a method for evaluating the effect of silicon (Si) impurity content on U-10Mo alloys. Si concentration in U-10Mo alloys has been shown to impact the following: volume fraction of precipitate phases, effective density of the final alloy, and  $^{235}\text{U}$  enrichment in the  $\gamma$ -UMo matrix. This report presents a model for calculating these quantities as a function of Si concentration, which along with fuel foil characterization data, will serve as a reference for quality control of the U-10Mo final alloy Si content. Additionally, detailed characterization using scanning electron microscope imaging, transmission electron microscope diffraction, and atom probe tomography analysis showed that Si impurities present in U-10Mo alloys form a Si-rich precipitate phase,  $\text{U}_2\text{Si}_2\text{MoC}$ . This newly discovered Si-rich phase is introduced in this document, as it significantly impacts how Si content affects final alloy microstructure and properties.



## Acronyms and Abbreviations

APT	atom probe tomography
BCC	body-centered cubic
C	carbon
EDS	energy dispersive spectroscopy
FA	final alloy
FFC	Fuel Fabrication Capability
HEU	highly enriched uranium
LEU	low-enriched uranium
Mo	molybdenum
SEM	scanning electron microscopy
Si	silicon
U	uranium
U-10Mo	uranium alloyed with 10 weight percent molybdenum
UC	uranium carbide
UMo	body-centered cubic $\gamma$ -uranium-molybdenum alloy
$^{235}\text{U}$ enrichment	weight of $^{235}\text{U}$ as a percentage of total weight of U



# Contents

Purpose and Scope .....	iii
Acronyms and Abbreviations .....	v
1.0 Introduction .....	1
2.0 Silicon Balance Model for Calculating Effective Density and Enrichment of the Final Alloy.....	2
2.1 Motivation for Silicon Balance Model Development .....	2
2.2 Si Balance Model Background.....	3
2.2.1 Overview .....	3
2.2.2 Assumptions .....	4
2.3 Step 1: Estimating the Number of U, Mo, C, and Si Atoms in UMo, UC, and U <sub>2</sub> Si <sub>2</sub> MoC Phase in the FA, per the FA Composition Specifications .....	4
2.4 Step 2: <sup>235</sup> U Enrichment in $\gamma$ -UMo Matrix as a Function of Si Concentration.....	5
2.5 Step 3: Estimating Densities of UMo Matrix, UC, and U <sub>2</sub> Si <sub>2</sub> MoC Phases.....	7
2.5.1 UMo Matrix.....	7
2.5.2 U <sub>2</sub> Si <sub>2</sub> MoC.....	7
2.5.3 UC .....	8
2.6 Step 4: Estimating the Volume Fractions of UMo, UC, and U <sub>2</sub> Si <sub>2</sub> MoC.....	8
2.7 Step 5: Estimating the Effective Density of the Final Alloy .....	9
3.0 Future Work.....	13
4.0 References .....	13

# Figures

1	Overall SEM Backscattered Electron Image of As-Cast and Homogenized U-10Mo Alloy Showing All Precipitates.....	2
2	Unit Cell of the $U_2Si_2MoC$ Phase .....	3
3	Enrichment of $^{235}U$ wt% in UMo Matrix of FA vs. Si Concentration, Assuming Two Different Cases .....	6
4	Volume Percentages of $U_2Si_2MoC$ and UC vs. Silicon Concentration in Final U-10Mo Alloy.....	9
5	Effective Density of Final Alloy Based on Rule of Mixtures as a Function of Si Concentration from 0 to 1000 ppm .....	10
6	Mo Concentration (in at%) in UMo Matrix as a Function of Si Concentration for Both Cases 1 and 2.....	11
7	Mo Concentration (in wt%) in UMo Matrix as a Function of Si Concentration for Cases 1 and 2....	12

# 1.0 Introduction

The U.S. Department of Energy, National Nuclear Security Administration's Office of Material Management and Minimization is developing monolithic metallic fuel to meet the objectives of the United States High Performance Research Reactor Program (USHPRR). The metallic fuel selected to replace current dispersed high-enriched uranium (HEU) fuels is a low-enriched uranium (LEU) 10-weight-percent (wt%) molybdenum alloy with less than 20 wt%  $^{235}\text{U}$ . The Fuel Fabrication (FF) pillar of the USHPRR has undertaken a series of activities in order to develop a fabrication process that will yield qualified fuel. A number of activities have been conducted in order to increase understanding of the effect of processing conditions on the final formed fuel microstructure. A variety of factors can directly affect the final U-Mo LEU alloy performance, including chemistry of raw materials (e.g., HEU plus a depleted U-Mo master alloy), the casting process (e.g., melting procedure, melt-mold and melt-gas interactions), and the thermomechanical processes used in fuel fabrication (e.g., hot and cold rolling, annealing). It has been determined that the final U-10Mo alloy microstructure (e.g. degree of phase transformation) and properties are influenced by amounts of impurities and the secondary phases that they form, such as uranium carbides (UC),  $\text{U}_2\text{Si}_2\text{MoC}$ , and oxides. These impurity and second-phase particles not only alter the transformation kinetics and may also form second phase particles with not only  $^{238}\text{U}$  but also  $^{235}\text{U}$  thus scavenging the matrix from  $^{235}\text{U}$ .

In work reported in a recent publication (Jana et. al 2017), it was observed that Si enrichment along  $\gamma$ -UMo grain boundaries is responsible for early onset of the phase transformation observed during sub-eutectoid annealing. Based on prior chemical analysis of UMo samples (Nyberg et. al 2015), Si is known to be an impurity element present in U-10Mo alloys. It is hypothesized that the UC and  $\text{U}_2\text{Si}_2\text{MoC}$  phases may be present in the HEU feedstock or could be formed during the melting and casting stages in U-Mo alloy preparation. Depending on when the UC and  $\text{U}_2\text{Si}_2\text{MoC}$  phases are formed, the  $^{235}\text{U}$  enrichment in these secondary phases and the U-Mo matrix can vary. Enrichment of the U-Mo matrix can also depend on the volume fraction of  $\text{U}_2\text{Si}_2\text{MoC}$ , which is in turn dependent on the Si concentration. Therefore, investigating the effect of varying Si content (in ppm) on the U-10Mo system is essential to better understanding how impurity content impacts phase transformation kinetics as a function of thermomechanical processing parameters. A model that can accurately predict final fuel microstructure and properties as a function of Si concentration is needed.

Prior work presented in Devaraj et al. (2016a) determined the effect of carbon concentration on the density of the final formed fuel. In this 2016 report, it was hypothesized that  $^{235}\text{U}$  could either remain in the  $\gamma$ -UMo matrix or form UC, thereby affecting final fuel microstructure, properties, and performance. A similar concept was adopted for development of the model presented here, in which different assumptions regarding scavenging of  $^{235}\text{U}$  are investigated.

The model presented in this work was developed to in order to estimate the following as a function of Si concentration:  $\text{U}_2\text{Si}_2\text{MoC}$  and UC volume fractions, effective density of the final U-10Mo alloy, and  $^{235}\text{U}$  enrichment in the U-Mo matrix.

This report is organized in the following manner: Section 2 presents the silicon balance model, including motivation and background, relevant equations, and results. Future Work is presented in Section 3, and all references cited are provided in Section 4.

## 2.0 Silicon Balance Model for Calculating Effective Density and Enrichment of the Final Alloy

### 2.1 Motivation for Silicon Balance Model Development

Based on detailed microstructure characterization results by scanning electron microscopy – energy dispersive spectroscopy (SEM-EDS), transmission electron microscopy (TEM), and atom probe tomography (APT) (Devaraj et al. 2016b), the as-cast and homogenized U-10Mo final alloy (FA) received from the Y-12 National Security Complex typically contains two impurity phases: uranium carbide (UC) and a Si-rich phase,  $U_2Si_2MoC$ . The newly discovered ( $U_2Si_2MoC$ ) phase has a tetragonal lattice, and the  $\gamma$ -UMo matrix has the body-centered cubic (BCC) structure. Hereafter, the  $\gamma$ -UMo matrix phase will be referred to as the UMo phase (Burkes et al. 2009, 2010; Joshi et al. 2015a, 2015b). Based on backscattered electron SEM images, the UMo phase appears light gray, whereas UC appears dark gray and  $U_2Si_2MoC$  appears black, as shown in Figure 1, below.

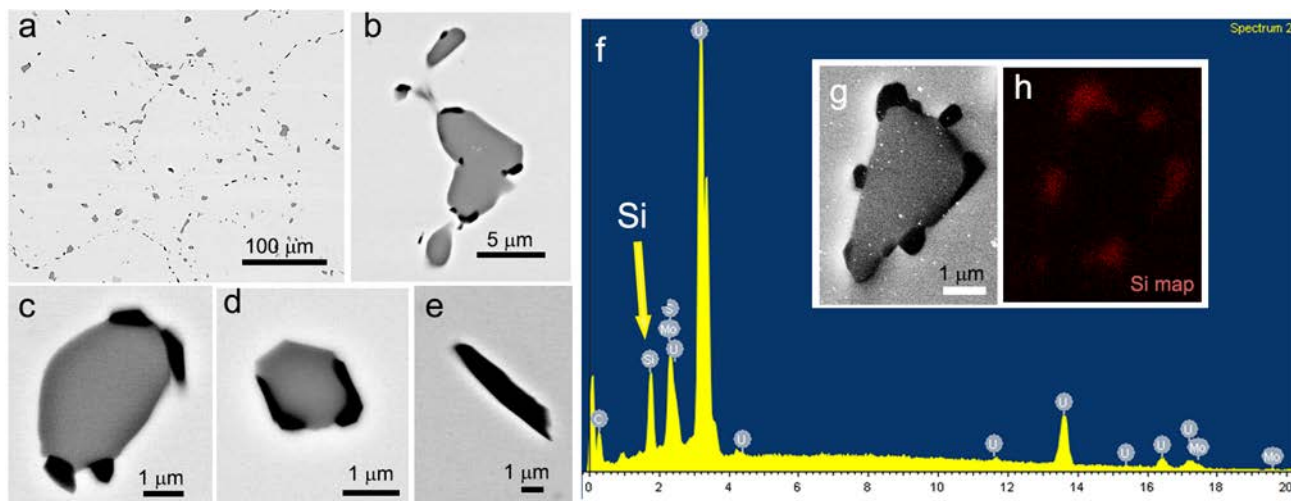


Figure 1. (a) Overall SEM Backscattered Electron Image of As-Cast and Homogenized U-10Mo Alloy Showing All Precipitates. (b–d) Coexisting UC precipitates (gray contrast) and  $U_2Si_2MoC$  precipitates (darker contrast). (e) Independent  $U_2Si_2MoC$  precipitates. (f) EDS spectrum from  $U_2Si_2MoC$  precipitate. (g) SEM-EDS mapping of a UC precipitate with  $U_2Si_2MoC$  precipitates around it. (h) Si map (red color) of the same structure shown in (g).

TEM analysis revealed the crystal structure of the newly discovered  $U_2Si_2MoC$  phase in the FA, which has not yet been reported in literature. The structure of this new phase as deduced from TEM and APT and verified with computational studies is shown in Figure 2, with corresponding space group and lattice parameters.

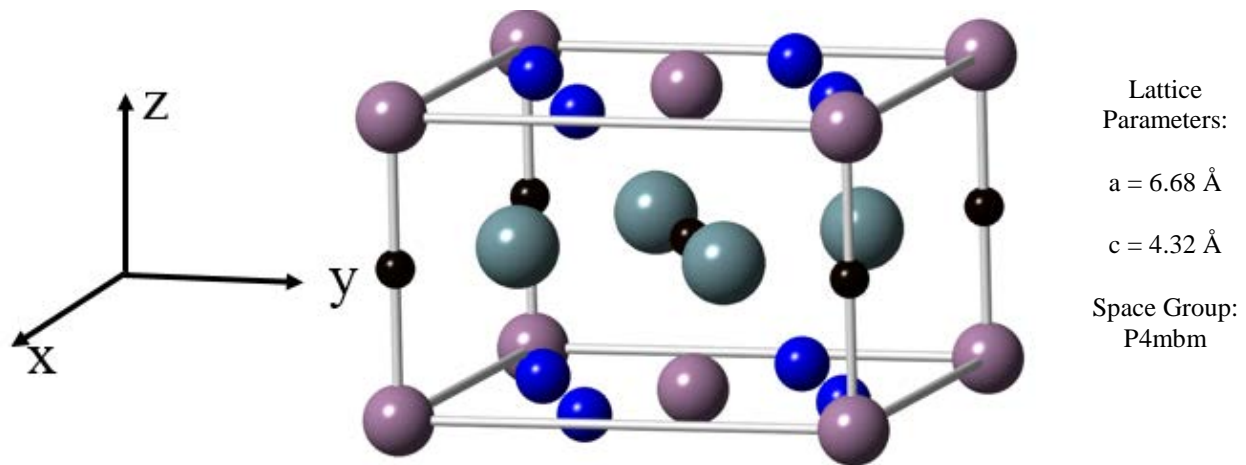


Figure 2. Unit Cell of the  $U_2Si_2MoC$  Phase. Per unit cell there are 4 U atoms (gray), 4 Si atoms (blue), 2 Mo atoms (purple), and 2 C atoms (black). Lattice parameters (a, c) and space group are indicated adjacent to the unit cell schematic.

The presence of  $U_2Si_2MoC$  in the FA has implications for properties of the FA due to its influence on mechanical processing and transformation kinetics. The presence of the  $U_2Si_2MoC$  phase directly affects final fuel microstructure; therefore it is important to be able to predict  $U_2Si_2MoC$  volume fraction as a function of Si concentration, where Si is a known impurity element in the FA. No model predicting volume fraction of a Si-rich phase as a function of Si concentration has been reported in literature; thus, a model was developed that links volume fraction of  $U_2Si_2MoC$  in the FA to Si concentration (from 0–500 ppm). This model, referred to as the “Si balance model” is presented here.

## 2.2 Si Balance Model Background

### 2.2.1 Overview

The goal of the Si balance model is to calculate the following as a function of Si concentration from 0–500 ppm:

1.  $^{235}U$  enrichment in  $\gamma$ -UMo matrix
2. volume percentages of UC and  $U_2Si_2MoC$  phases
3. effective density of the FA
4. Mo concentration in the  $\gamma$ -UMo matrix.

All of the quantities listed above are presented as plots in this report in order to observe trends in these quantities with increasing Si concentration.

In order to calculate the above quantities, the following major steps were completed; they are subsequently detailed in this report (with all calculations provided in the accompanying Excel worksheet, named “Si\_balance\_calculations\_June2017”):

1. Step 1: Estimate the number of  $^{235}U$ ,  $^{238}U$ , Mo, C, and Si atoms in the UMo matrix, UC phase, and  $U_2Si_2MoC$  phase in the FA, per FA composition specifications.
2. Step 2: Estimate  $^{235}U$  enrichment in  $\gamma$ -UMo matrix as a function of Si concentration.

3. Step 3: Estimate densities of UMo matrix, UC phase, and  $U_2Si_2MoC$  phase.
4. Step 4: Estimate the volume fraction of UMo matrix, UC phase, and  $U_2Si_2MoC$  phase.
5. Step 5: Estimate the effective density of the FA.

## 2.2.2 Assumptions

All calculations were done for 1000 g of FA, and the following assumptions were made:

1. FA composition is  $U_{89.9-y}Mo_{10}C_{0.1}Si_y$ , with 19.75 wt% of total U as  $^{235}U$  (19.75 wt% enrichment). Based on the FA composition listed here, we are assuming the amounts of Mo and C are fixed, whereas the amounts of Si and U in the FA vary.
2. The solubility of C in the UMo matrix is zero.
3. C is partitioned between UC and  $U_2Si_2MoC$  phases. Carbon in the FA is used to form  $U_2Si_2MoC$  first, with the remaining C in UC. The UC volume fraction varies with Si concentration in the FA.
4. All the C atoms in the FA form UC, where C concentration is fixed at 1000 ppm (1 g out of the total 1000 g alloy mass).
5. The solubility of Si in the UMo matrix is zero. All Si in the FA is in the  $U_2Si_2MoC$  phase.
6. Two different bounding assumptions are made for where  $^{235}U$  is located in the FA. These assumptions were made in order to obtain lower and upper bounds of enrichment in the  $\gamma$ -UMo matrix. These two assumptions, referred to as Case 1 and Case 2, respectively, are described below:
  - a. Case 1: All U in UC and  $U_2Si_2MoC$  phases is  $^{235}U$ . All remaining  $^{235}U$  in FA is in the UMo matrix.
  - b. Case 2: All U in UC and  $U_2Si_2MoC$  is  $^{238}U$ . All  $^{235}U$  is in UMo matrix.
7. UMo matrix density is calculated based on the mass and volume per unit cell of the  $\gamma$ -UMo BCC structure.
  - a. Mass per unit cell is calculated by multiplying the atomic percentages of  $^{235}U$ ,  $^{238}U$ , and Mo atoms by the 2 atoms per unit cell.
  - b. The volume of a single unit cell is calculated from the theoretical unit cell parameter,  $a$ , assuming the hard sphere model.
8. The UMo matrix density varies with  $^{235}U$  enrichment; thus, because of Assumption 6, the matrix density varies as a function of Si concentration. UMo matrix density is not assumed to be constant, as was previously assumed in Devaraj et al. (2016a).
6. Based on the above assumptions, the mass of each element in 1000 g of FA was estimated for a range of Si concentrations from 0 to 500 ppm. The concentration of Si expected in the FA is up to 500 ppm.

## 2.3 Step 1: Estimating the Number of U, Mo, C, and Si Atoms in UMo, UC, and $U_2Si_2MoC$ Phase in the FA, per the FA Composition Specifications

The total number of atoms of  $^{235}U$ ,  $^{238}U$ , Mo, C, and Si in the FA was calculated for different values of Si concentration from 0–500 ppm, given the mass of the element (in grams), Avogadro's number (atoms/mol), and atomic mass (grams/mol), as seen in Equation 1.

In many equations included in this report, units are listed in brackets next to the corresponding parameter.

$$\text{Number of atoms of an element} = \frac{\text{weight of element [g]} \times 6.023 \times 10^{23} \left[ \frac{\text{atoms}}{\text{mol}} \right]}{\text{atomic mass} \left[ \frac{\text{g}}{\text{mol}} \right]} \quad (1)$$

Next, the number of atoms per phase was calculated for UMo, UC, and U<sub>2</sub>Si<sub>2</sub>MoC.

In order to estimate the number of atoms per phase, the distribution of U, Mo, C, and Si was considered.

C partitioning between the Si-rich phase (U<sub>2</sub>Si<sub>2</sub>MoC) and UC is accounted for in this model by assuming C is first allocated to the Si-rich phase, and then all remaining C in the FA (per FA composition specifications) is in the UC phase. We also assume all Si in the FA is in U<sub>2</sub>Si<sub>2</sub>MoC, and then calculate the number of Si atoms in this phase. Then we calculate the number of C atoms in U<sub>2</sub>Si<sub>2</sub>MoC by dividing the total number of Si atoms in this phase by 2 (since the ratio of C:Si atoms is 1:2). C content in the FA is constant, so all remaining C is assumed to be in UC. The total number of atoms in each phase was calculated based on the number of Si atoms for Si concentrations varying from 0 to 500 ppm. The basic equations used to calculate total number of atoms in each phase are provided in Equations 2–4, below:

$$\begin{aligned} \text{Total number of atoms in UMo phase} \\ = [\#U \text{ atoms in FA} - (\#U \text{ atoms in UC} + \#U \text{ atoms in U}_2\text{Si}_2\text{MoC})] \\ + (\#Mo \text{ atoms in FA} - \#Mo \text{ atoms in U}_2\text{Si}_2\text{MoC}) \end{aligned} \quad (2)$$

$$\text{Total number of atoms in UC phase} = (\#C \text{ atoms in FA} - \#C \text{ atoms in U}_2\text{Si}_2\text{MoC}) * 2 \quad (3)$$

$$\begin{aligned} \text{Total number of atoms in U}_2\text{Si}_2\text{MoC phase} \\ = (2 * \text{Total number of Si atoms}) + (2 * \frac{1}{2} * \text{number of Si atoms}) \end{aligned} \quad (4)$$

## 2.4 Step 2: <sup>235</sup>U Enrichment in $\gamma$ -UMo Matrix as a Function of Si Concentration

As previously reported in Devaraj et al. (2016a), the fuel specification nominally requires a 19.75 wt% enrichment of <sup>235</sup>U in the FA, the bulk of which comes from the HEU feedstock. The UC and U<sub>2</sub>Si<sub>2</sub>MoC phases may be present in the HEU feedstock, or they could be formed during the melting and casting stages in the UMo alloy preparation. Depending on when the UC and U<sub>2</sub>Si<sub>2</sub>MoC phases are formed, the <sup>235</sup>U enrichment in these secondary phases and the UMo matrix can vary. The enrichment of the UMo matrix can also depend on the volume fraction of U<sub>2</sub>Si<sub>2</sub>MoC, which is in turn dependent on the Si concentration.

Here, the enrichment of <sup>235</sup>U in the UMo matrix is calculated for two limiting cases, as previously presented in the Assumptions section (2.2.2) of this report (and listed below for clarity):

Case 1: All uranium in UC and U<sub>2</sub>Si<sub>2</sub>MoC is <sup>235</sup>U.

Case 2: All uranium in UC and U<sub>2</sub>Si<sub>2</sub>MoC is <sup>238</sup>U.

Case 1 and Case 2 are assumed to be two extremes; the actual matrix enrichment is expected to fall in between the enrichment values calculated for these two assumptions.

Enrichment of the UMo matrix is plotted for Case 1 and Case 2 in Figure 3, below:

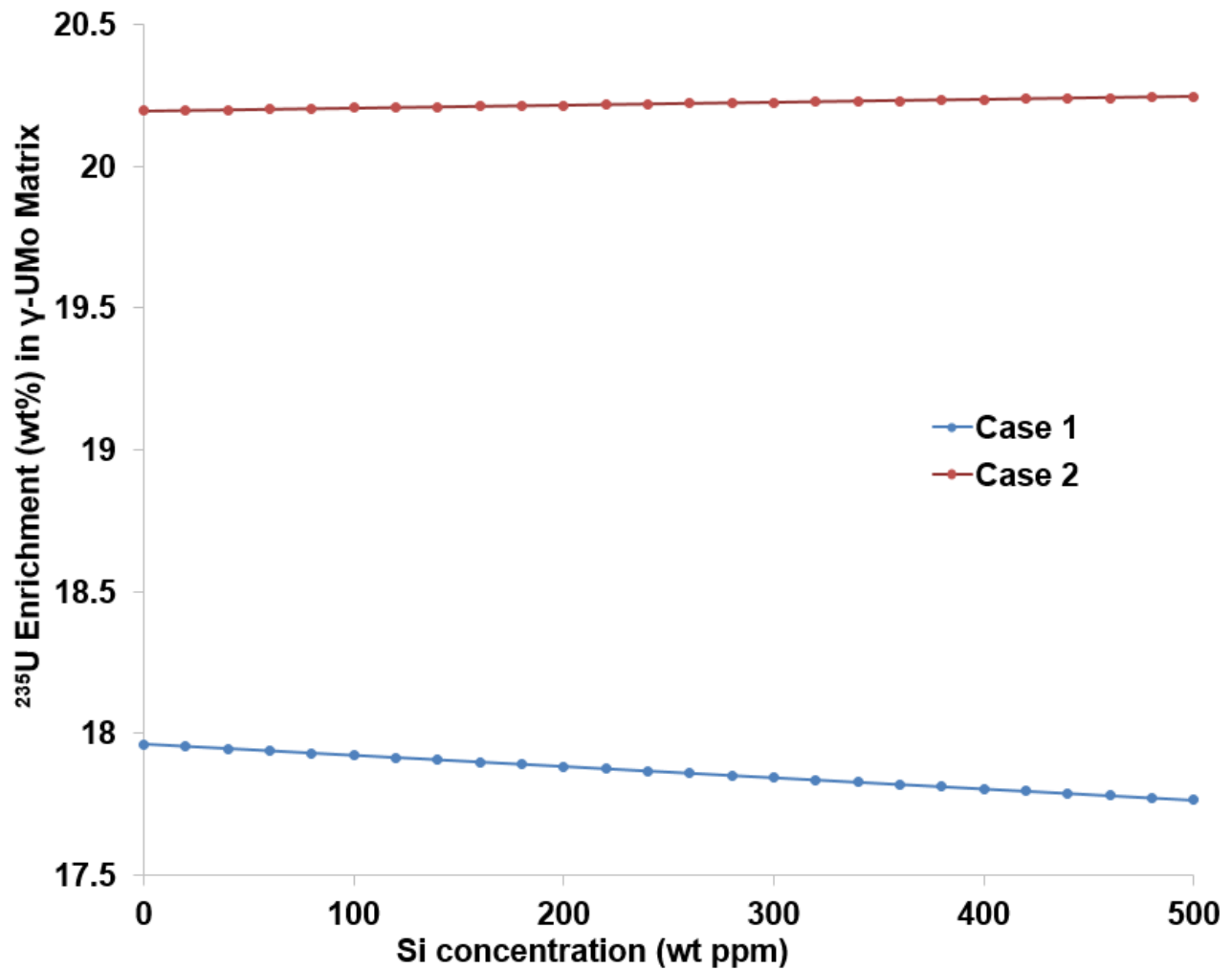


Figure 3. Enrichment of  $^{235}\text{U}$  wt% in UMo Matrix of FA vs. Si Concentration, Assuming Two Different Cases. (Case 1) All Uranium in UC and  $\text{U}_2\text{Si}_2\text{MoC}$  is  $^{235}\text{U}$ , and (Case 2) All Uranium in UC and  $\text{U}_2\text{Si}_2\text{MoC}$  is  $^{238}\text{U}$ .

Enrichment of the UMo matrix is lower in Case 1 than in Case 2 because in Case 1, the U in the UC and  $\text{U}_2\text{Si}_2\text{MoC}$  phases is assumed to be  $^{235}\text{U}$ , which means there is less  $^{235}\text{U}$  in the UMo matrix, resulting in a lower enrichment. As Si concentration increases, matrix enrichment decreases in Case 1 and increases in Case 2, which again occurs due to the initial assumptions of where  $^{235}\text{U}$  is allocated in the FA. In Case 1, since all U in UC and  $\text{U}_2\text{Si}_2\text{MoC}$  is assumed to be  $^{235}\text{U}$ , as Si concentration increases, there are more Si atoms in the  $\text{U}_2\text{Si}_2\text{MoC}$  phase, and thus there are more  $^{235}\text{U}$  atoms in this phase, and fewer in the UMo matrix, which results in decreasing enrichment with increasing Si concentration. For Case 2, since no  $^{235}\text{U}$  is in the UC and  $\text{U}_2\text{Si}_2\text{MoC}$  phases, as Si concentration increases, more  $^{238}\text{U}$  is allocated to UC and  $\text{U}_2\text{Si}_2\text{MoC}$ , leaving a higher enrichment of  $^{235}\text{U}$  in the UMo matrix.

## 2.5 Step 3: Estimating Densities of UMo Matrix, UC, and U<sub>2</sub>Si<sub>2</sub>MoC Phases

Next, densities of each phase were calculated for Case 1 and Case 2. Different densities were calculated for each case because the molecular weights of <sup>238</sup>U and <sup>235</sup>U are different, and although there may be the same number of U atoms per unit cell in each phase, the density will vary based on number of <sup>235</sup>U or <sup>238</sup>U atoms per unit cell. Additionally, the density of the UMo matrix was calculated as a function of Si concentration, because the enrichment varies with increasing Si concentration.

### 2.5.1 UMo Matrix

In order to calculate density of the  $\gamma$ -UMo matrix, weight percentages of <sup>235</sup>U, <sup>238</sup>U, and Mo in the matrix were converted to atomic percentages. Next, the total mass per unit cell was calculated, and finally, density was calculated given the total mass per unit cell and the volume per unit cell. Equations 5–7 (below) were used in the matrix density calculation. The same approach was applied for both Case 1 and Case 2.

$$\text{Volume of a } \gamma\text{UMo unit cell [cm}^3\text{]} = a_0^3 \quad (5)$$

*Mass of  $\gamma$ UMo unit cell*

$$\begin{aligned} &= \left[ \frac{\text{at\% } U^{235}}{100} * \frac{2 \text{ atoms}}{\text{unit cell}} * \frac{U^{235} \text{ g}}{\text{mol}} * \frac{\text{mol}}{6.022^{23} \text{ atoms}} \right] \\ &+ \left[ \frac{\text{at\% } U^{238}}{100} * \frac{2 \text{ atoms}}{\text{unit cell}} * \frac{U^{238} \text{ g}}{\text{mol}} * \frac{\text{mol}}{6.022^{23} \text{ atoms}} \right] \\ &+ \left[ \frac{\text{at\% } Mo}{100} * \frac{2 \text{ atoms}}{\text{unit cell}} * \frac{Mo \text{ g}}{\text{mol}} * \frac{\text{mol}}{6.022^{23} \text{ atoms}} \right] \end{aligned} \quad (6)$$

$$\text{Density of UMo Matrix} = \frac{\text{total grams in } \gamma\text{UMo unit cell [g]}}{\text{volume of a } \gamma\text{UMo unit cell [cm}^3\text{]}} \quad (7)$$

UMo matrix density varies with Si concentration from 17.283 to 17.288 g/cm<sup>3</sup> for Case 1, and 17.275 to 17.284 g/cm<sup>3</sup> for Case 2. It is noted here that the effective density of the  $\gamma$ -UMo matrix with 19.75 wt% <sup>235</sup>U was previously calculated to be 17.33 g/cm<sup>3</sup> (constant) as is detailed in Devaraj et al. (2016a). The UMo matrix density calculated in this report is generally in agreement with that which was previously calculated; however, in this work, we account for variation of the matrix density with <sup>235</sup>U enrichment, which is the reason for the small variation in calculated density values between the 2016 report and this work.

### 2.5.2 U<sub>2</sub>Si<sub>2</sub>MoC

U<sub>2</sub>Si<sub>2</sub>MoC has a tetragonal lattice with 12 atoms per unit cell (4 U atoms, 4 Si atoms, 2 Mo atoms, and 2 C atoms).

To estimate the mass of a unit cell of U<sub>2</sub>Si<sub>2</sub>MoC, the masses of 4 U atoms, 4 Si atoms, 2 Mo atoms, and 2 C atoms are added, as shown below in Equation 7, where the U molecular weight variable here is either 238.0285 g/mol for <sup>238</sup>U or 235.04 for <sup>235</sup>U.

From the lattice parameters of U<sub>2</sub>Si<sub>2</sub>MoC (a = 6.68 Å, c = 4.32 Å), the volume of a unit cell is calculated using Equation 8 and then used to estimate the density of U<sub>2</sub>Si<sub>2</sub>MoC using Equations 9–10:

$$\text{Volume of a } U_2Si_2MoC \text{ unit cell [cm}^3] = a^2 * c \quad (8)$$

$$\begin{aligned} \text{Mass of a } U_2Si_2MoC \text{ unit cell [g]} \\ = \frac{4 \frac{\text{atoms}}{\text{unit cell}} \times [\text{U molecular weight } \frac{\text{g}}{\text{mol}}]}{6.023 \times 10^{23} \text{ atoms/mol}} + \frac{4 \frac{\text{atoms}}{\text{unit cell}} \times 28.0855 \text{ g/mol}}{6.023 \times 10^{23} \text{ atoms/mol}} \\ + \frac{2 \frac{\text{atoms}}{\text{unit cell}} \times 95.96 \text{ g/mol}}{6.023 \times 10^{23} \text{ atoms/mol}} + \frac{2 \frac{\text{atoms}}{\text{unit cell}} \times 12.011 \text{ g/mol}}{6.023 \times 10^{23} \text{ atoms/mol}} \end{aligned} \quad (9)$$

$$\text{Density of } U_2Si_2MoC \left[ \frac{\text{g}}{\text{cm}^3} \right] = \frac{\text{Mass of a } U_2Si_2MoC \text{ unit cell}}{\text{Volume of } U_2Si_2MoC \text{ unit cell}} \quad (10)$$

The two densities calculated for the  $U_2Si_2MoC$  phase for Case 1 and Case 2 are  $10.93 \text{ g/cm}^3$  and  $11.03 \text{ g/cm}^3$ , respectively.

### 2.5.3 UC

Similar to the density calculations performed for the  $U_2Si_2MoC$  phase, UC density was calculated by first calculating the volume of the unit cell, given lattice parameter (a), and the mass of the unit cell. Volume, mass, and density were calculated using Equations 11–13, below:

$$\text{Volume of a UC cell [cm}^3] = a^3 \quad (11)$$

$$\text{Mass of a UC unit cell [g]} = \frac{4 \frac{\text{atoms}}{\text{unit cell}} \times [\text{U molecular weight } \frac{\text{g}}{\text{mol}}]}{6.023 \times 10^{23} \text{ atoms/mol}} + \frac{4 \frac{\text{atoms}}{\text{unit cell}} \times 12.011 \text{ g/mol}}{6.023 \times 10^{23} \text{ atoms/mol}} \quad (12)$$

$$\text{Density of UC} \left[ \frac{\text{g}}{\text{cm}^3} \right] = \frac{\text{Mass of a UC unit cell}}{\text{Volume of UC unit cell}} \quad (13)$$

The two densities calculated for Case 1 and Case 2 are  $13.44 \text{ g/cm}^3$  and  $13.60 \text{ g/cm}^3$ , respectively. The density of  $^{235}\text{UC}$  was estimated to be  $13.4394 \text{ g/cm}^3$  in Devaraj et al. (2016a), which is consistent with calculations reported here.

## 2.6 Step 4: Estimating the Volume Fractions of UMo, UC, and $U_2Si_2MoC$

The volume fraction of each phase was calculated, given the total number of atoms per phase, volume per atom in each phase, and the total volume of all phases in the FA, as shown in Equation 14:

$$\text{volume fraction of phase} = \frac{\text{number of atoms in phase} * \text{volume per atom of a phase}}{\text{total volume of all phases}} \quad (14)$$

In order to understand how the volume fractions of the Si-rich phase and UC vary with increasing Si concentration, the volume percentages (volume fraction multiplied by 100) of these phases were plotted versus Si concentration from 0 to 500 ppm (Figure 4).

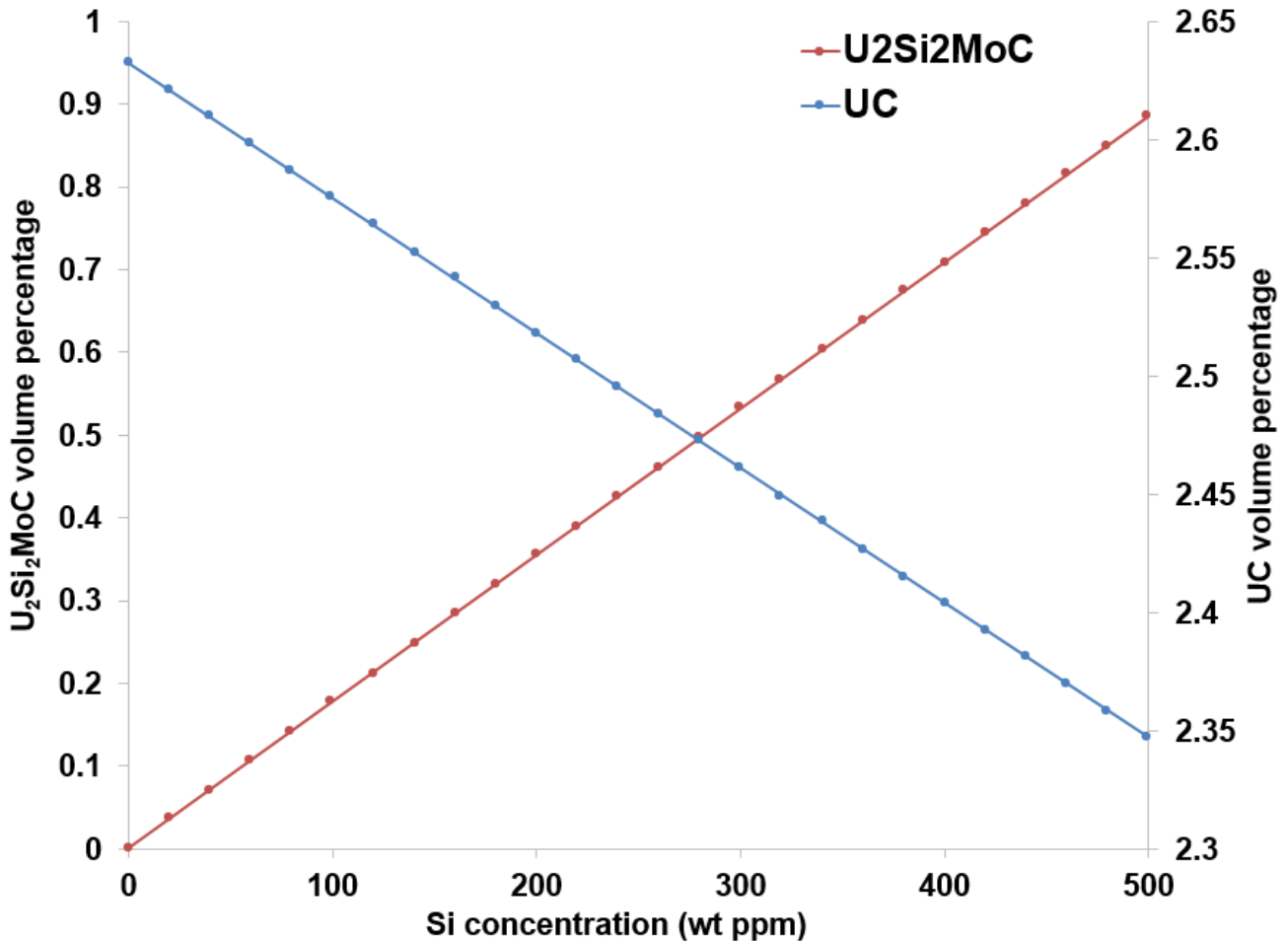


Figure 4. Volume Percentages of U<sub>2</sub>Si<sub>2</sub>MoC and UC vs. Silicon Concentration in Final U-10Mo Alloy

As Si concentration increases, the volume percent of U<sub>2</sub>Si<sub>2</sub>MoC increases, because all Si in the FA is in this phase. Because C content is fixed, the UC volume percent must decrease, since as Si concentration increases, more C is needed to form this Si-rich phase, meaning less C is available to form UC.

## 2.7 Step 5: Estimating the Effective Density of the Final Alloy

Here, effective density of the FA was calculated as a function of Si concentration for Case 1 and Case 2.

By using the calculated individual phase densities of each of the phases (detailed above in Step 3), and the volume fraction of each phase, the effective density of the FA was estimated by the rule of mixtures, provided below in Equation 15:

$$\begin{aligned}
 & \text{Effective density of final alloy} \\
 & = (\text{Density of UC} \times \text{Volume fraction of UC}) \\
 & + (\text{Density of UMo phase} \times \text{Volume fraction of } \gamma\text{UMo})
 \end{aligned} \tag{15}$$

$$+ (\text{Density of } U_2Si_2MoC \text{ phase} \times \text{Volume fraction of } U_2Si_2MoC)$$

The variation in density as a function of silicon concentration is given in Figure 5 for the two cases considered to estimate the upper and lower bound for FA density.

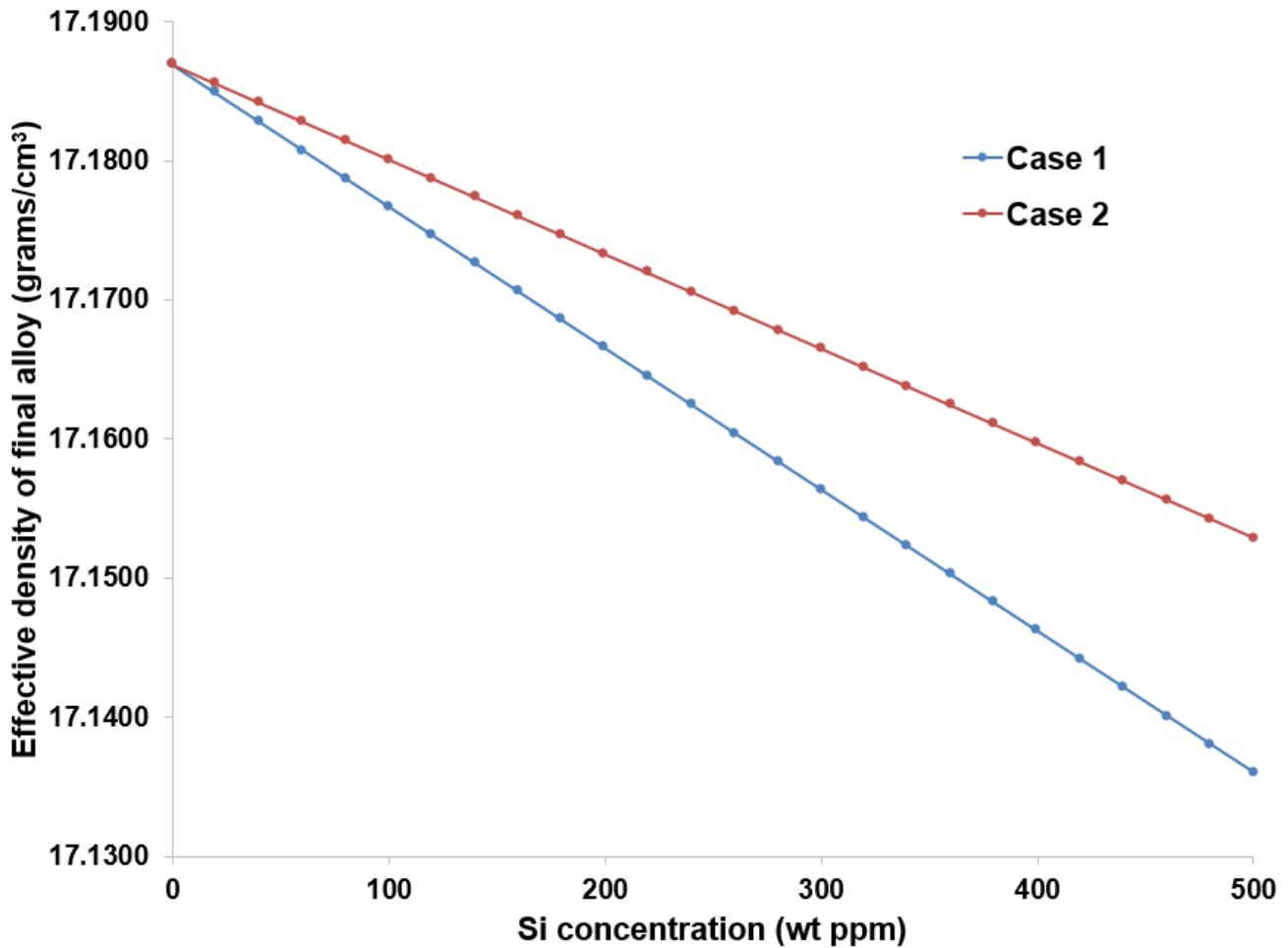


Figure 5. Effective Density of Final Alloy Based on Rule of Mixtures as a Function of Si Concentration from 0 to 1000 ppm. Case 1 assumes that all U in UC and  $U_2Si_2MoC$  is  $^{235}U$  and Case 2 assumes that all U in UC and  $U_2Si_2MoC$  is  $^{238}U$ .

Additionally, based on the total number of atoms found in Step 1, the Mo concentration in the UMo matrix was also calculated as a function of Si concentration. The final Mo concentration in UMo matrix was first calculated in atomic percent by taking a ratio of the number of Mo atoms remaining in the UMo matrix after formation of  $U_2Si_2MoC$  and UC phases to the total number of all atoms in the UMo matrix. Here, we assume the only atoms in the matrix are U and Mo. Figure 6 and Figure 7 show change in Mo in atomic percent and weight percent, respectively, in the UMo matrix as a function of Si concentration up to 500 ppm. Concentration of Mo was first calculated in atomic percent, then converted to weight percent because Mo concentration related to UMo fuels is typically reported in weight percent, and the Mo weight percent in the UMo matrix varies for Case 1 in comparison to Case 2.

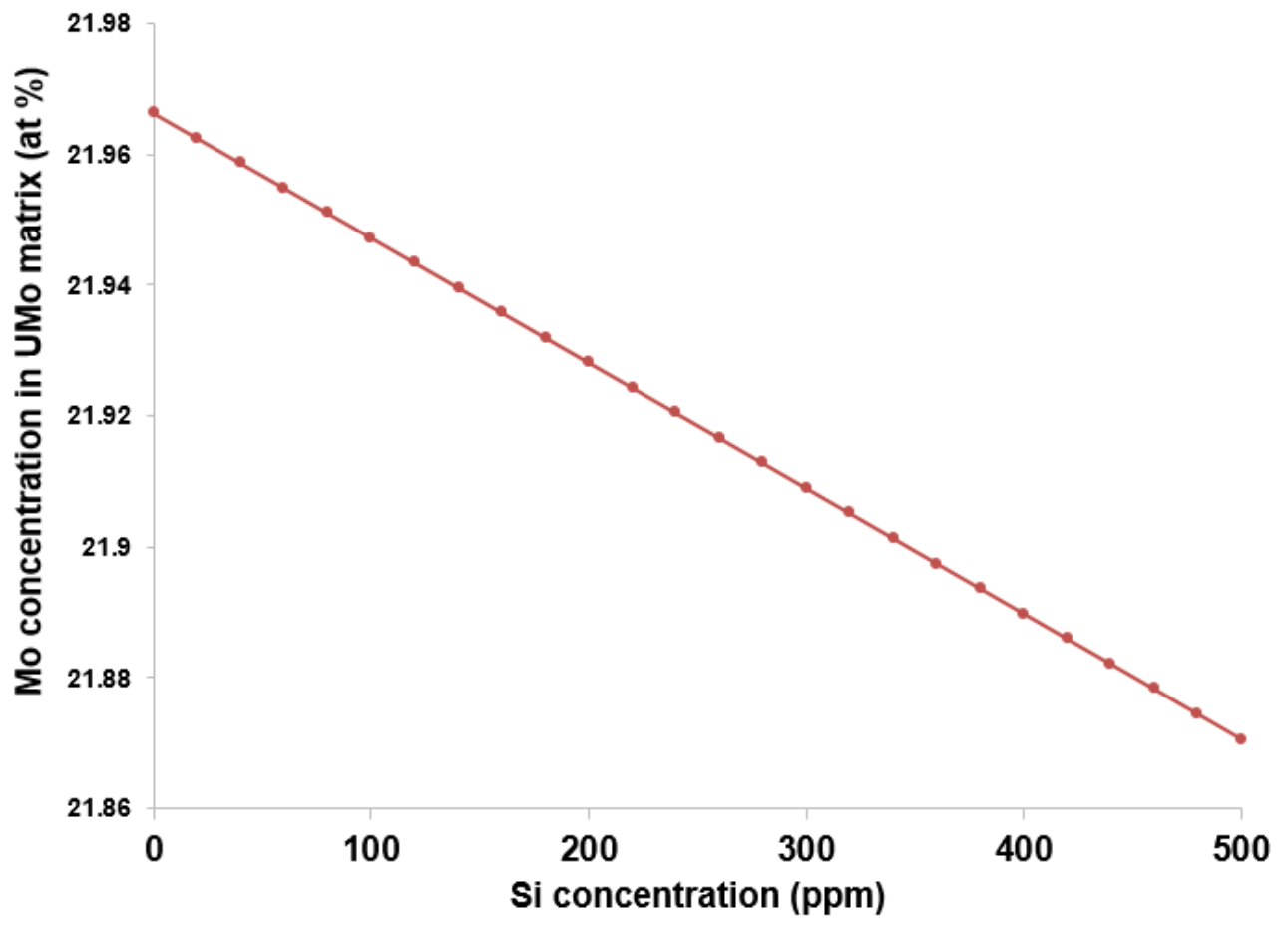
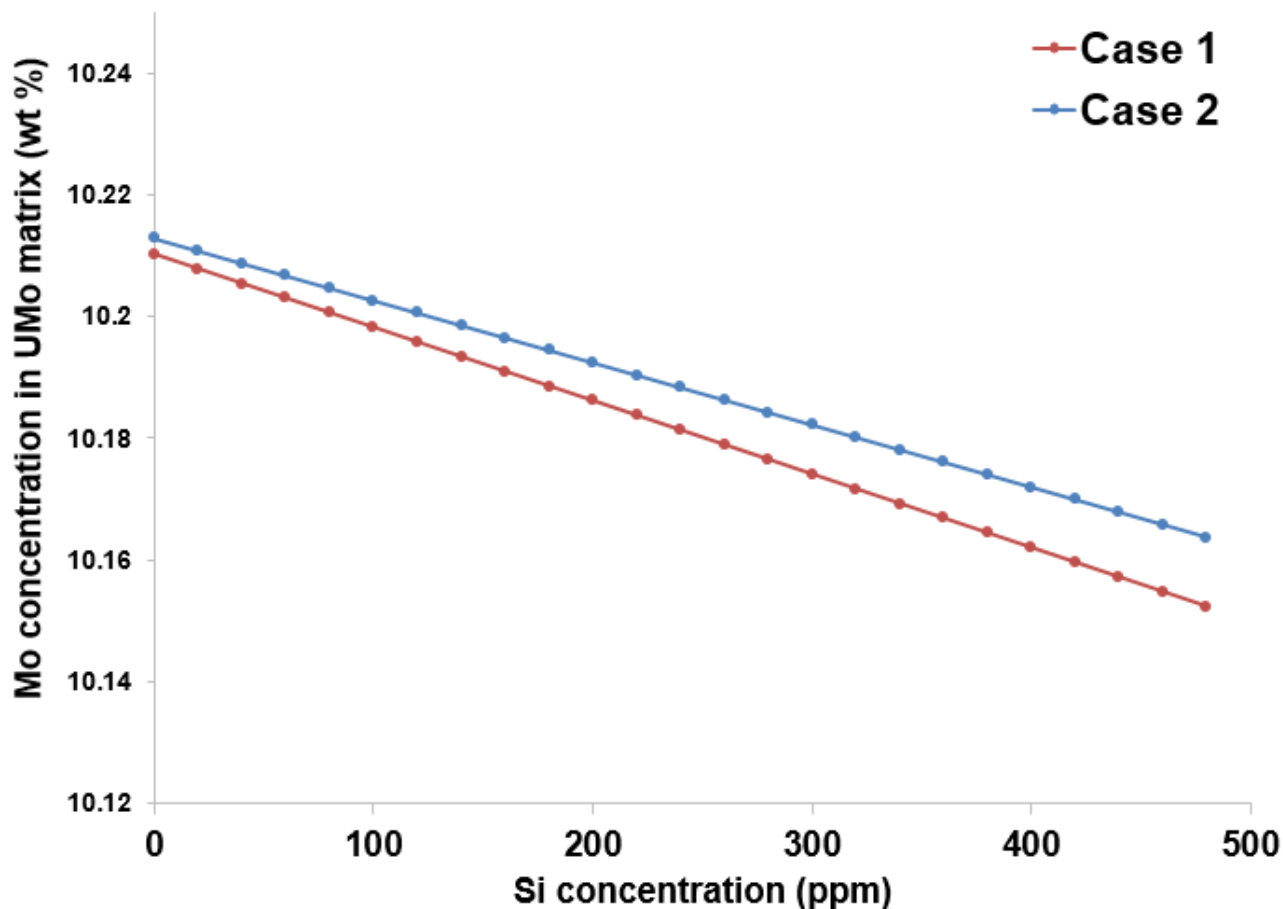


Figure 6. Mo Concentration (in at%) in UMo Matrix as a Function of Si Concentration for Both Cases 1 and 2.



**Figure 7.** Mo Concentration (in wt%) in UMo Matrix as a Function of Si Concentration for Cases 1 and 2.

Figure 6 and Figure 7 both illustrate the general trend that as Si concentration increases, the Mo concentration in the UMo matrix decreases. This observed trend is expected because as Si ppm increases, more Mo atoms are needed to form the  $U_2Si_2MoC$  phase, which means there are fewer Mo atoms in the UMo matrix. When atomic percent is converted to weight percent, the Mo concentration varies between Case 1 and Case 2 because the amount of  $^{235}U$  and  $^{238}U$  in the UMo matrix is different.

For Case 1, all the U in second phases (UC and  $U_2Si_2MoC$ ) is assumed to be  $^{235}U$ , which has a lower molecular weight than  $^{238}U$ . As the Si content increases, Mo and  $^{235}U$  are needed to form  $U_2Si_2MoC$  in a ratio of 1:2 (number of Mo atoms to number of  $^{235}U$  atoms). Therefore, the weight of U in the matrix decreases, the entire weight of the matrix decreases, and the weight of Mo in the matrix decreases. This trend is observed for Case 2 as well; however Mo weight percent is lower than for Case 1 due to the fact that in Case 2 there is less  $^{238}U$  in the matrix (since all the U in second phases is assumed to be  $^{238}U$ ), and thus the overall weight of the matrix is lower, and continues decreasing as Mo atoms are needed to form the Si-rich phase.

It is also noted that the Mo concentration in the UMo matrix calculated here will deviate from the expected 10 wt% (21.57 at%) with increasing Si concentration.

When there is no Si in the FA, the Mo concentration in the matrix is higher than the FA composition of 10 wt% (21.57 at%) Mo due to the presence of 1000 ppm C, which forms UC, thereby reducing the total U atoms in matrix and in turn increasing the atomic percentage of Mo.

Supplementary Information: The worksheet with the all calculations is provided in the accompanying Excel file, named “Si\_balance\_calculations\_June2017.”

### 3.0 Future Work

The key motivation for this fundamental microstructure characterization work is that microstructure is linked to properties of the UMo fuel. At this time, better understanding of what and how microstructural features develop and how they are linked to properties (such as swelling) is important work to ultimately improve predictive capabilities linking properties to microstructure.

Future work will be focused on fundamental materials characterization of the UMo system in order to understand how the microstructure of this material system changes as a function of impurity element concentration (in particular, Si and C), and processing parameters such as time and temperature.

Specifically, we will investigate experimentally how the volume fraction of  $U_2Si_2MoC$  phase varies in the depleted uranium-molybdenum (DUMo) alloys as a function of homogenization temperature and time. We will investigate results of various homogenization times at 900°C and 1000°C. We have obtained evidence that with homogenization at 1000°C, the larger  $U_2Si_2MoC$  phase dissolves and thin plate-like precipitates of the same phase are formed. These observed microstructure changes also appeared to retard the time-temperature-transformation (TTT) kinetics during sub-eutectoid annealing treatments. We will investigate how the homogenization treatment temperature and time can be optimized to control the transformation extent in UMo alloys.

### 4.0 References

Burkes D, T Hartmann, R Prabhakaran, and J-F Jue. 2009. “Microstructural characteristics of  $DU-xMo$  alloys with  $x = 7-12$  wt%.” *Journal of Alloys and Compounds* 479:140–147. Accessed July 24, 2017, at <http://www.sciencedirect.com/science/article/pii/S0925838808022627>.

Burkes D, R Prabhakaran, T Hartmann, J-F Jue, and F Rice. 2010. “Properties of  $DU-10$  wt% Mo alloys subjected to various post-rolling heat treatments.” *Nuclear Engineering and Design* 240:1332–1339. Accessed July 24, 2017, at <http://www.sciencedirect.com/science/article/pii/S0029549310001184>.

Devaraj A, R Prabhakaran, EJ McGarrah, VV Joshi, SY Hu, and CA Lavender. 2016a. *Theoretical Model for Volume Fraction of UC,  $^{235}U$  Enrichment, and Effective Density of Final U-10MO Alloy*. PNNL SA 117284, Pacific Northwest National Laboratory, Richland, Washington. Accessed July 24, 2017, at [http://www.pnnl.gov/main/publications/external/technical\\_reports/PNNL-SA-117284.pdf](http://www.pnnl.gov/main/publications/external/technical_reports/PNNL-SA-117284.pdf).

Devaraj A, VV Joshi, S Manandhar, CA Lavender, L Kovarik, S Jana, and BW Arey. 2016b. *High Resolution Characterization of UMo Alloy Microstructure*. PNNL-SA-26020, Pacific Northwest National Laboratory, Richland, Washington. Accessed July 24, 2017, at [http://www.pnnl.gov/main/publications/external/technical\\_reports/PNNL-26020.pdf](http://www.pnnl.gov/main/publications/external/technical_reports/PNNL-26020.pdf).

Joshi V, E Nyberg, C Lavender, D Paxton, and D Burkes. 2015a. “Thermomechanical process optimization of U-10wt% Mo – Part 2: The effect of homogenization on the mechanical properties and microstructure.” *Journal of Nuclear Materials* 465:710–718. Accessed July 24, 2017, at <http://www.sciencedirect.com/science/article/pii/S002231151530091X>.

Joshi V, E Nyberg, C Lavender, D Paxton, H Garmestani, and D Burkes. 2015b. “Thermomechanical process optimization of U-10 wt% Mo – Part 1: High-temperature compressive properties and microstructure.” *Journal of Nuclear Materials* 465:805–813. DOI: 10.1016/j.jnucmat.2013.10.065. Accessed July 24, 2017, at <http://www.sciencedirect.com/science/article/pii/S0022311513012312?via%3Dihub>.

Jana S, A Devaraj, L Kovarik, B Arey, L Sweet, T Varga, C Lavender, and V Joshi. “Kinetics of cellular transformation and competing precipitation mechanisms during sub-eutectoid annealing of U10Mo alloys.” *Journal of Alloys and Compounds* Volume 723, 2017, Pages 757-771, ISSN 0925-8388, DOI: 10.1016/j.jallcom.2017.06.292. Accessed July 24, 2017, at <http://www.sciencedirect.com/science/article/pii/S0925838817323009?via%3Dihub>.

Nyberg EA, DE Burkes, VV Joshi, and CA Lavender. 2015. *The Microstructure of Rolled Plates from Cast Billets of U-10Mo Alloys*. PNNL-24160, Pacific Northwest National Laboratory, Richland, WA. Accessed July 24, 2017, at [http://www.pnnl.gov/main/publications/external/technical\\_reports/PNNL-24160.pdf](http://www.pnnl.gov/main/publications/external/technical_reports/PNNL-24160.pdf).





**Pacific Northwest**  
NATIONAL LABORATORY

*Proudly Operated by **Battelle** Since 1965*

902 Battelle Boulevard  
P.O. Box 999  
Richland, WA 99352  
1-888-375-PNNL (7665)

U.S. DEPARTMENT OF  
**ENERGY**

---

[www.pnnl.gov](http://www.pnnl.gov)